Sorption and diffusion behavior of actinium(III) ions in contact with hydroxyapatite as a transporter of medical radionuclides

A. V. Severin,[a]★ A. N. Vasiliev,[a,b] A. V. Gopin,[a] and K. I. Enikeev[a]

[a]Chemistry Department, M. V. Lomonosov Moscow State University, Build. 3, 1 Leninskie Gory, 119991 Moscow, Russian Federation. E-mail: severinal@yandex.ru
[b]Institute for Nuclear Research, Russian Academy of Sciences, 27 ul. Fizicheskaya, Troitsk, 108840 Moscow, Russian Federation

The sorption of the actinium(III) ions as ^{225,228}Ac isotopes on hydroxyapatite (HAP) with various textures was studied. A "reverse" generator using an extraction chromatographic sorbent based on diglycolamide derivative (DGA Resin) was proposed for ^{228}Ac production. The chemical yield of the product was ≥90%. The optimal acidity of the solution during sorption (pH 6—7) and the ratio of solid and liquid phases (20 mg of the sorbent per mL of the solution) were determined in preliminary experiments. The process kinetics is adequately described by pseudo-second-order model. The stationary state is reached rapidly (in 10 min) when a HAP suspension is used, whereas time (20—30 min) is needed for textured samples. The possibility of actinium ion diffusion within the bulk of these samples is shown. The diffusion coefficient of actinium estimated by diffusion in a wet HAP paste layer (one-dimensional model) was $(1.0\pm0.2)\cdot10^{-7}$ cm^2 s^{-1}.

Key words: hydroxyapatite, actinium, radionuclide, sorption kinetics, diffusion, texture.

Medical research carried out in the last two decades demonstrated a huge potential of the alpha-therapy of cancer and extensive opportunities offered by using various approaches to the delivery of alpha-emitters to cancer cells.[1] In recent years, out of the possible radionuclides that can be used for this purpose, ^{225}Ac ($\tau_{1/2}$ = 9.9 days), together with ^{213}Bi ($\tau_{1/2}$ = 46 min), a decay product of ^{225}Ac, have come to the forefront owing to their nuclear-physical properties.[2,3]

For example, encouraging results were obtained in the clinical trials of ^{225}Ac-PSMA-617 (prostate-specific membrane antigen) for the treatment of metastatic prostate cancer.[4,5] Actinium-225-containing radiopharmaceuticals are under trials for the treatment of leukemia, glioma, and neuroendocrine tumors, with the total number of patients exceeding 500.[6]

In recent years, accelerator systems for large-scale production of this radionuclide have been put into operation in several world centers in Russia,[7,8] United States,[9] and Canada.[10] The most studied method for ^{225}Ac production is isolation from proton-irradiated natural thorium (^{232}Th)[11,12] or ^{226}Ra (on cyclotrons).[13]

A radionuclide can be characterized by a specific pharmacokinetics suitable for the therapy. For example, ^{223}Ra has clear-cut organotropism; therefore, it was the first alpha emitter to be clinically used for the therapy of bone metastases.[14] However, in the vast majority of cases, it is attached to a delivery vector. This vector can be represented by either small molecules or peptides,[15] lipisomes,[16] and other nanoparticles.[17] Brachytherapy in which a large sealed source of radiation is placed into the body can be considered as a limiting case.[18] Other materials tested as transporters for therapeutic and diagnostic radionuclides include modified particles of gold,[19] iron oxide,[20] lanthanum phosphate,[21] silica gel,[22] polymers,[23] and other particles with various sizes. Hydroxyapatite (HAP), the main bone tissue matrix, also proved to be applicable. It is fully biocompatible and has a number of properties making it superior to other materials. Indeed, HAP labeled with beta-emitters, such as ^{90}Y,[24] ^{177}Lu,[25] and ^{153}Sm,[26] is used in radiosynovectomy, with the medication being administered intravenously. In addition, HAP demonstrated high sorption properties towards the following heavy metal cations: Pb^{II}, Zn^{II}, Co^{II}, and Zr^{IV}.[27—29]

Hydroxyapatite has been studied [30—33] as a transporter for alpha-emitting radionuclides such as ^{223}Ra, ^{213}Bi, and ^{211,212}Pb. As we showed previously,[34,35] the sorption of radium is fast and high sorption efficiency is attained over a broad pH range; furthermore, after heat treatment, the desorption of radium in an isotonic solution is minor. The use of this sorbent as a transporter for triply charged $^{225}Ac^{III}$ ion may also be promising.

Since there is still no routine industrial manufacture of ^{225}Ac in a quantity sufficient for all consumers, in this

Published in Russian in *Izvestiya Akademii Nauk. Seriya Khimicheskaya,* No. 12, pp. 2286—2293, December, 2020.
1066-5285/20/6912-2286

study, some of the experiments were carried out with a more readily available ^{228}Ac isotope, which can be isolated from a ^{232}Th salt. In the literature, there is no procedure suitable for developing an efficient generator for short-lived actinium based on extraction chromatography sorbents.

This study had several goals. First, it was planned to investigate the generator process for the production of ^{228}Ac from thorium nitrate salt and to evaluate the efficiency of this isotope generator and product purity. The next step was to study sorption of actinium on HAP under various conditions (pH, phase ratio, contact time, HAP morphology) and the diffusion behavior of actinium in the textured sorbent, *i.e.*, the sorbent characterized by a particular arrangement and size of structural units of the solid phase, which form a hierarchical system of pores in the sample bulk.

Experimental

Production of actinium-228. The short-lived ^{228}Ac isotope (analog of the medical ^{225}Ac isotope) was produced on a regular basis using the "reverse" $^{228}Ra/^{228}Ac$ generator. The ^{228}Ra parent isotope isolated from a natural thorium salt existing in equilibrium with daughter decay products. The salt was dissolved in nitric acid, and the macroquantities of initial thorium were separated by liquid—liquid extraction (LLE) with di(2-ethylhexyl) phosphoric acid (D-2-EHPA) in toluene repeated three times (Fig. 1). As shown in our previous study,[36] the composition of the aqueous phase most appropriate for separation of thorium selectively with respct to actinium is 1—8 *M* HNO_3; hence, in this work, we used 6 *M* HNO_3.

A thorium-232 nitrate solution with a concentration of 0.4 mol L^{-1} (300 mL) was prepared. The age of thorium nitrate exceeded 50 years. Macroquantities of the initial thorium were separated by threefold extraction from the nitric acid solution with D-2-EHPA (Sigma—Aldrich, USA; agitation with an equal amount of a toluene solution (1 : 1) on a shaker for 20 min).

It was found that the nitric acid solution of ^{228}Ra obtained upon thorium separation is unsuitable for direct use in the generator, because of breakthrough of actinium, apparently due to the presence of heavy metal impurities in the initial salt. Therefore, radium was additionally purified using extraction chromatography with the sorbent based on crown-6-ether derivative (Sr Resin, Triskem Int., France). Radium has high retention factor in 3 *M* perchloric acid ($k' = 100$)[37] and can be selectively sorbed by Sr Resin even from salt solutions. The desorption of $^{224,228}Ra$ was performed by dilute nitric acid.

The aqueous phase containing $^{228}Ra/^{228}Ac$ and, presumably, stable impurities was evaporated to dryness, and the residue was dissolved in 3 *M* $HClO_4$. The resulting solution was passed through a column with a sorbent based on 18-crown-6 ether derivative (Sr Resin, Triskem Int., France), the column was washed with 3 *M* $HClO_4$, then ^{228}Ra was desorbed with 0.1 *M* nitric acid, and the eluate was concentrated and dissolved in 5 mL of 4 *M* HNO_3.

After that, the obtained solution was kept for accumulating ^{228}Ac, and actinium was collected from 4 *M* nitric acid by extraction chromatography with a diglycolamide sorbent (DGA Resin, Triskem Int., France). Under these conditions, actinium had the highest retention factor ($k' = 10^3$),[7] while radium was not virtually sorbed.

Each elution was carried out in the following way. The initial solution was passed through a column (with 2 cm height and 1 mL total volume) packed with the sorbent. Then the column was washed with 10 mL of 4 *M* HNO_3, and 3—5 mL of ^{228}Ac was desorbed with 0.01 *M* HNO_3.

Bismuth-212 present in the initial solution was retained on the column and was not desorbed with 0.01 *M* nitric acid, while ^{212}Pb remained in the initial solution, because it has no affinity for the sorbent from 4 *M* nitric acid.

The column was washed with 4 *M* HNO_3 for the next elution. After each elution, the initial solution was mixed with the first portion of wash solution (1 mL) to minimize the loss of the parent radionuclide.

This procedure gave the product with high radiochemical purity. The yield of ^{228}Ac was more than 90% with allowance for the decay. After the decay of actinium, no ^{228}Ac was found in the eluate by a repeated measurement. The recorded γ-spectra and known formulas[36] were used to calculate the minimum detectable ^{228}Ra activity, which corresponded to the radionuclide purity of the obtained product of ≥99.98% relative to the initial activity. Despite the fact that after each elution, the solution volume increased due to addition of the portion of the wash solution (1 mL), high actinium retention factors allowed conducting up to 20 elutions without preconcentration of the initial

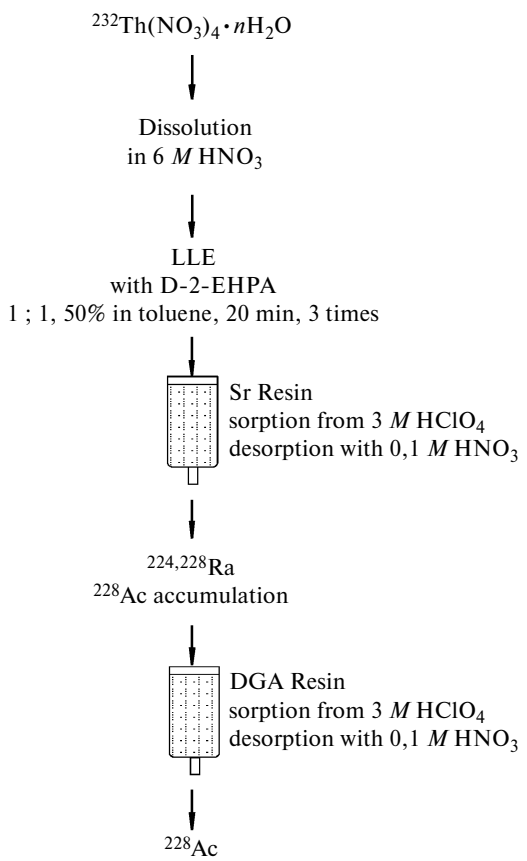

Fig. 1. Diagram of ^{228}Ac isotope production from a natural thorium salt.

solution. The subsequent preconcentration can be performed on a column with Sr Resin, as indicated above.

Production of actinium-225. The ^{225}Ac radionuclide was obtained by irradiation of a natural thorium metal target with medium energy protons (90—120 MeV) at the Institute for Nuclear Research, Russian Academy of Sciences (Troitsk), and isolated and purified as a solution in nitric acid by a known procedure.[7] Immediately before diffusion measurements, an aliquot portion of the solution was concentrated, the residue was dissolved in 0.01 *M* HNO_3, and the solution was neutralized with 0.1 *M* NaOH to pH ≈ 5—7.

Preparation and characterization of the sorbent. Nanodispersed HAP materials, an aqueous suspension (5 wt %) of HAP and a powder derived from the suspension (HAP-0), were used as the main sorbents. These sorbents were prepared according to the standard procedure described in detail earlier.[38,39] Samples of HAP-0 powder pretreated at 1100 °C for 3—4 h in a MIMP furnace (Russia) (HAP_T) were also used. This material possessed enhanced strength and low porosity and relatively small specific surface area (~35—40 $m^2\ g^{-1}$).[40] One more sorbent was prepared from HAP-0 suspension and subjected to thermally stimulated morphological selection to form spherical granules (HAP_{sph}).[41] All types of sorbents were characterized by powder X-ray diffraction and electron microscopy (SEM and TEM); and the specific surface area of the sorbents was measured using the thermal desorption of nitrogen.

Identification of the optimal conditions of sorption. The pH value of the sorption medium and the weight (total active surface area) of the sorbent were chosen as the parameters for identifying the optimal sorption conditions. The sorption experiments were carried out with the ^{228}Ac isotope, which was isolated and purified as described above. It served as the analog of the medical ^{225}Ac isotope. For studying sorption as a function of pH of the mother liquor, 200 μL-portions of radionuclide-labeled solution were added into ten 5 mL vials and diluted with distilled water. Each solution was adjusted to the required pH value (1—11) by adding 0.01 and 0.1 mol L^{-1} aqueous solutions of NaOH. The total sample volume was now 2 mL. Into each vial, HAP-0 (30 mg) was added, and the mixtures were agitated on a shaker for 1 h and centrifuged at 2000 *g* for 1 min. For activity measurements by γ-spectrometry (γ-spectrometer with a GR3818 Canberra Ind. high-purity Ge-detector (USA)), 1.5 mL samples of the mother liquor were taken.

The dependence of the ^{228}Ac sorption on the sorbent weight was studied using HAP-0 powder samples at pH 6.3. Samples weighing 2, 10, 20, 50, 100, and 150 mg were placed into 5-mL vials containing 2 mL of the liquid phase (200 μL of ^{228}Ac solution and 1.8 mL of H_2O). Samples were agitated on a shaker for 1 h. After completion of sorption, the mother liquor was separated, as described above, and 1.5 mL samples were taken for activity measurement by γ-spectrometry.

Sorption and desorption kinetics. The kinetics of ^{228}Ac sorption on HAP was studied at pH 6.4 for all types of sorbents. During the experiment, ten samples with a volume of 2 mL (200 μL of ^{228}Ac solution and 1.8 mL of H_2O) were prepared, equal amounts of the sorbent (40 mg of HAP) were added, and the samples were agitated on a shaker for specified periods of time. Then the solid and liquid phases were separated, and the activity was measured for 1.5 mL of the mother liquor.

For studying the ^{228}Ac desorption kinetics, sorption was first carried out for 1 h by the procedure described above. Seven samples were prepared (the volume of the liquid phase and the sorbent weight (HAP-0 powder) were the same as in the study of the sorption kinetics). The solid and liquid phases were separated by centrifugation for 1 min at 2000 *g*. After that, the mother liquor was removed and replaced by a 0.9% NaCl solution. The obtained mixture was agitated on a shaker for the following periods of time: 3, 5, 10, 15, 30, 60, and 120 min. After completion of these time periods, the phases were separated, and 1.5 mL portions of the solution were taken for activity measurements.

Diffusion experiments. The diffusion parameters of the radionuclides in the wet HAP-0 paste were measured using a special cell (Fig. 2, *a*) and the ^{225}Ac radionuclide. The cell was manufactured by 3D printing (Flashforge Dreamer 3D printer with a 100 μm resolution) of temperature- and acid-resistant SBS

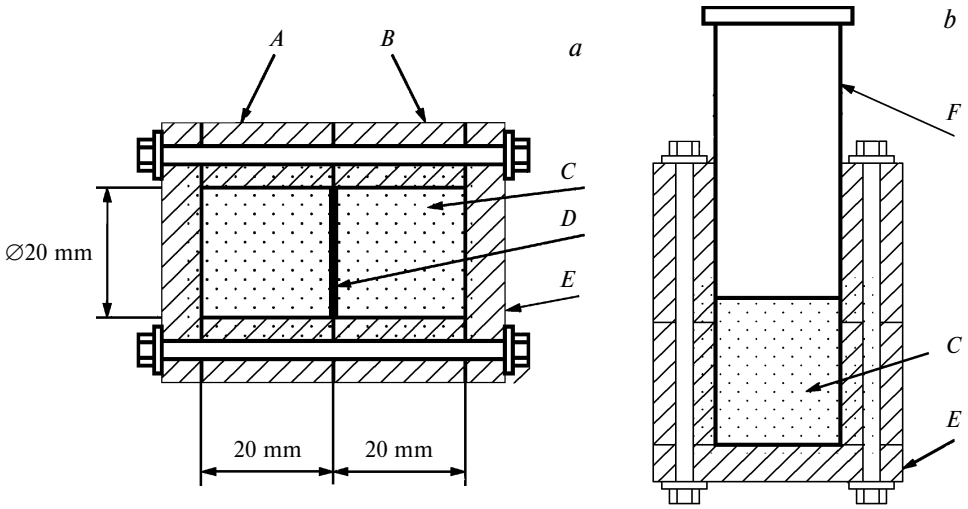

Fig. 2. Diagram of the diffusion cell for experiment (*a*) and for compaction of the HAP paste (*b*). The designation of radionuclide position corresponds to the time of its addition; *A* and *B* are halves of the cell, *C* is HAP paste, *D* is radionuclide, *E* is the cell cover, *F* is screw piston.

plastic (FDPlast, Russia). The joints between the key units were sealed with special rubber gaskets.[42]

Using a screw piston, the halves of the cell were densely filled with the prepared HAP paste (Fig. 2, *b*). The excess of the paste was removed. In order to exclude the formation of the residual air voids, both halves were kept in a layer of distilled water for 24 h. After removal of excess water, a solution containing actinium-225 label was introduced on the inner surface of one of the cell halves, the inner part of the second half was pressed against it, and then the cell was tightly screwed (see Fig. 2, *a*), mounted in a horizontal position, and kept for 16 days. A 50 μL actinium label had a volumetric activity of 1 MBq mL^{-1}. Then the cell was dismantled, the cover of each half was removed, and a screw piston was mounted in place of the cover. With the piston, portions of HAP paste containing the radionuclide were squeezed out and partitioned. The portions of the paste were placed into 20 mL vials, weighed, and dissolved in equal minimum amounts of concentrated nitric acid; the activities of the resulting solutions were determined by γ-spectrometry (the ^{225}Ac counting rate was determined from the counting rate of the daughter ^{221}Fr ($\tau_{1/2}$ = 4.9 min; energy of gamma-quanta used to determine the nuclide, E_γ = 218.0 keV; probability of formation of these gamma-quanta, p = 11.44%) after the samples were kept for at least 50 min). All experiments were carried out at 22±2 °C.

Results and Discussion

Sorbent characterization demonstrated that all samples used in the study represented pure HAP as evidenced by powder X-ray diffraction data. The initial suspension particles were plate-like nanocrystals with average size of 100×30×10 nm. Upon aggregation, these particles were arranged into various hierarchical textures, depending on the method of pretreatment of the suspension or the suspension-derived powder, which differed in porosity and specific surface area (Table 1).

Optimization of ^{228}Ac sorption conditions. In the selection of process parameters and in kinetic experiments, the extent of actinium sorption was calculated using the formula

$$Q\,(\%) = (1 - A_{solv}/A_0) \cdot 100\%,$$

where A_{solv} and A_0 are the activities of 1.5 mL of the solution after and before sorption, respectively. The dependence of the percentage of actinium sorption by HAP on the pH of the mother liquor is shown in Fig. 3. Complete sorption occurs at pH >4. This type of dependence is characteristic[43] of sorption of trivalent metal cations by

Table 1. Specific surface area and porosity of the sorbent

Sample	Condition	$S_{sp}/m^2\ g^{-1}$	Porosity (%)
HAP-0(susp.)	Aqueous suspension	~350—400 (calculation)	—
HAP-0(powd.)	Powder	70—75	60—65
HAP_T	Calcined powder	35—40	20—25
$ГАП_{sph}$	Spherical granules	70—75	60—65

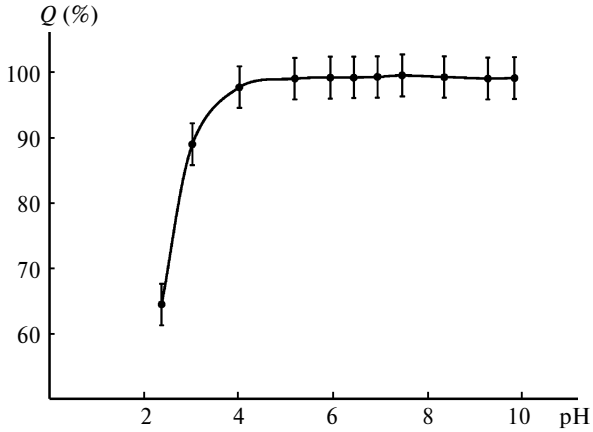

Fig. 3. Extent of actinium sorption (Q) as a function of pH of the mother liquor; the sorption duration is 1 h.

different structural forms of HAP. For the subsequent experiments, the pH range of the mother liquor was chosen to be 6—7.

One more parameter of the sorption to be optimized was the solid sorbent/liquid sorbate ratio, that is, the concentration of sorption sites interacting with the target substance from the mother liquor. The dependence obtained for this purpose is shown in Fig. 4. As can be seen from the plot (see Fig. 4), the sorption of actinium ions reaches a maximum of 98±2% when the total available surface area of the nanoparticle solid phase exceeds 20.4 mg mL^{-1} (4 $m^2\ mL^{-1}$). Thus, the optimal phase ratio is 20 mg of the sorbent per mL of the solution (40 mg per 2 mL).

The sorption kinetics of actinium-228 on various sorbent samples is shown in Fig. 5. The dynamic equilibrium of actinium in the solution—sorbent system is attained rapidly: within the first 10 min for HAP-0 suspension (~95% of actinium is sorbed); for other forms of sorbent, the stationary state is attained within 20—30 min.

The kinetic dependences were analyzed using well-known pseudo-first- and pseudo-second-order models.[44] When the experimental data were processed in the framework of the pseudo-first-order kinetic model, linearization was performed using the equation

$$\ln(q_e - q_t) = \ln(q_e) - k_1 t,$$

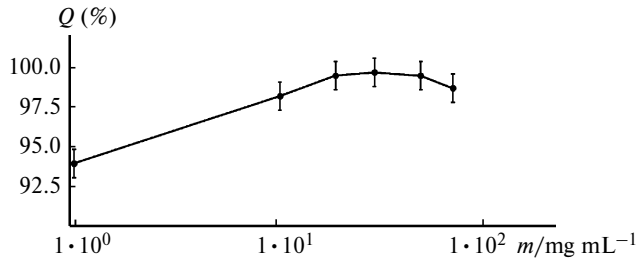

Fig. 4. Extent of actinium sorption (Q) as a function of the sorbent weight; the sorption duration is 1 h, pH 6.4.

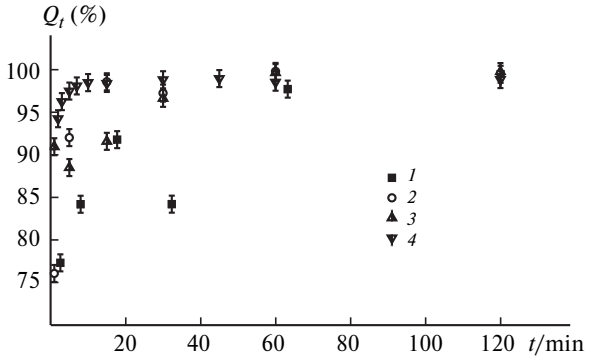

Fig. 5. Kinetics of sorption of ^{228}Ac on various HAP samples: HAP_T (*1*), HAP_{sph} (*2*), HAP-0(powd.) (*3*), and HAP-0(susp.) (*4*); pH 6.7.

where q_e and q_t are the equilibrium sorption and sorption at time t, k_1 is the first-order rate constant of sorption. By substituting the percentage of sorption $Q_t = q_t/q_e$, we have

$$\ln(1 - Q_t) = -k_1 t.$$

The approximation parameters for this model are given in Table 2. The rate constant of sorption calculated in terms of this model is maximum for the suspension and minimum for the annealed HAP powder, which is consistent with sorption curves (see Fig. 5). However, in view of the poor correlation parameters (R^2 <0.93 for any of the samples), the pseudo-first-order kinetic model should be considered unsuitable for describing the sorption of actinium on various HAP materials.

When the experimental data were processed in terms of the pseudo-second-order kinetic model, linearization was performed using the equation

$$\frac{t}{q_t} = \frac{1}{k_2 q_e^2} + \frac{1}{q_e} t,$$

where k_2 is the second-order rate constant of sorption. By substituting the extent of sorption Q_t by q_t/q_e, we get

$$\frac{t}{Q_t} = \frac{1}{k_2 q_e} + t.$$

The dependences approximated by this model are depicted in Fig. 6. The approximation parameters and the calculated $k_2 q_e$ values are summarized in Table 2. They are seen to increase in the series HAP_T < HAP-0(powd.) < HAP_{sph} < HAP-0(susp.), which is consistent with the sorption kinetic curves (see Fig. 5).

Analysis of the kinetic dependences also included a test for the possibility of actinium diffusion within HAP particles. Here we used the Weber—Morris model.[45] Plotting the dependences of q_t on $t^{0.5}$ usually gives a set of straight lines. The steps in the plot (Fig. 7) indicate the presence of several stages of the process.[46,47] The first stage is the external surface adsorption, or instantaneous adsorption. The second stage is gradual adsorption, the rate of which is limited by the rate of internal diffusion. The third stage is approaching the ultimate equilibrium where the diffusion within the particles starts to slow down due to the extremely low concentration of the sorbate.[48] It can be seen that diffusion within the particles affects the sorption in the calcined HAP powder and spherical HAP granules. In the case of dried HAP powder and HAP suspension, there are no signs internal diffusion. However, it may still matter, if a sorbent layer rather than single particles are considered.

Desorption of actinium from HAP-0 nanoparticles in physiological saline is depicted in Fig. 8 as a kinetic dependence. The amount desorpbed was calculated using the equatio

$$D = [1 - (A^2_{solv} - A^1_{solv})/(A_0 - A^1_{solv})] \cdot 100\%,$$

where A_0 is the activity of 1.5 mL of actinium solution before sorption; A^1_{solv} is the activity of 1.5 mL of the solution after sorption; A^2_{solv} is the activity of 1.5 mL of the solution after desorption. After the contact of labeled HAP particles with isotonic solution for 1 h, about 7—8% of the introduced actinium is desorbed. After HAP was labeled, it was subjected to modification. As a rule, this is done by means of various coatings that increase the particle stability and biocompatibility. For example, the HAP surface can be coated with polyethylene glycol (PEGylation),[49] chitosan,[50] or other polymers.[51] Due to ultralow concentration of actinium, sorption of even a therapeutic dose of active ^{225}Ac does not change the HAP surface (the maximum tolerable dose of the ^{225}Ac-DOTATOC agent[52] is ~40 MBq, or less than 10^{-10} mol), and the particles can

Table 2. Experimental parameters of kinetics of actinium sorption on HAP calculated by the pseudo-first- and pseudo-second-order kinetic models

Sample	Pseudo-first-order model		Pseudo-second-order model		
	k_1/min^{-1}	R^2	$1/(k_2 q_e)$/min	$k_2 q_e$/min^{-1}	R^2
HAP_T	0.05±0.01	0.85742	2.0±0.8	0.5±0.2	0.99791
HAP_{sph}	0.11±0.02	0.89934	0.4±0.1	2.6±0.8	0.99986
HAP-0(powd.)	0.10±0.02	0.92627	0.6±0.2	1.6±0.5	0.99987
HAP-0(susp)	0.7±0.1	0.90793	0.132±0.007	7.5±0.4	0.99998

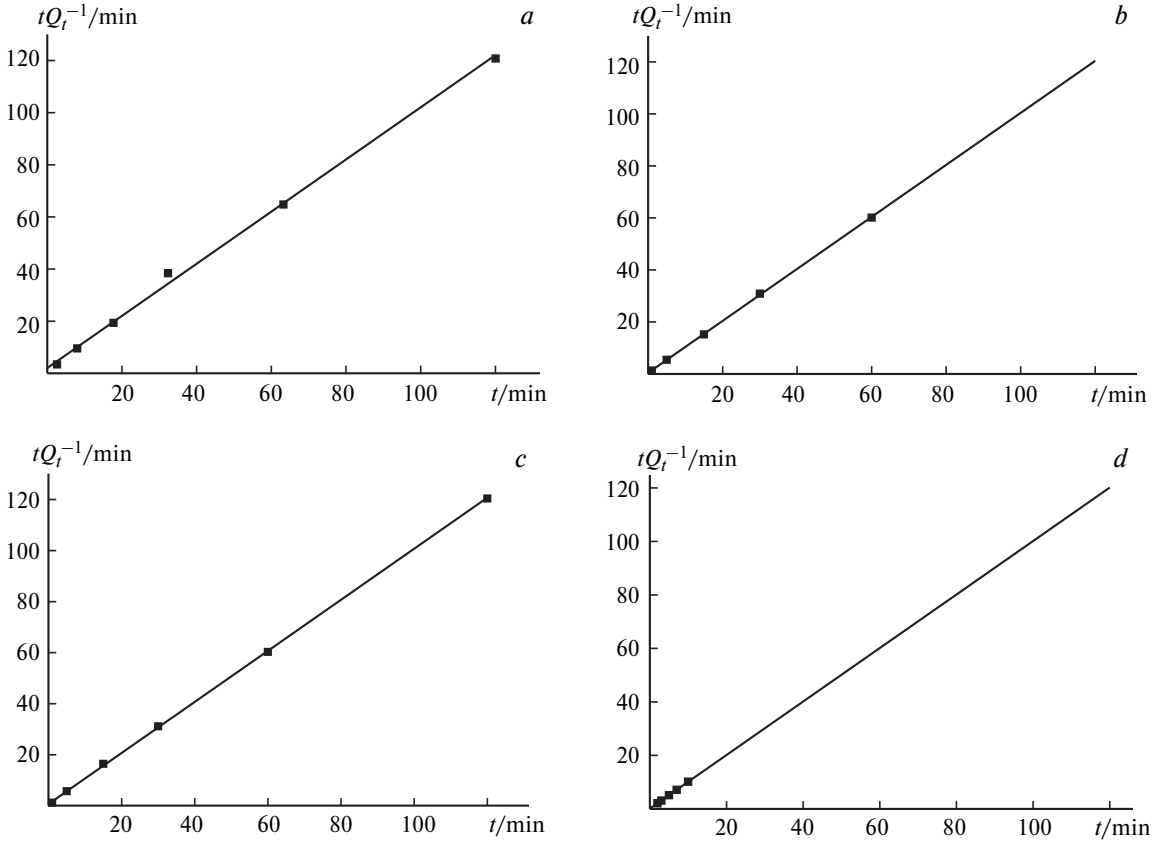

Fig. 6. Kinetics of actinium sorption on various HAP samples approximated using the pseudo-second-order kinetic model: HAP_T (*a*), HAP_{sph} (*b*), HAP-0(powd.) (*c*), and HAP-0(susp.) (*d*).

be modified after labeling to obtain the final radiopharmaceutical.

Calculation of the diffusion coefficient in a layer of wet HAP paste (^{225}Ac). One-dimensional unsteady diffusion is described by Fick′s second law

$$\frac{\partial C(x,t)}{\partial t} = \frac{\partial}{\partial x}\left[D(x,t)\frac{\partial C(x,t)}{\partial x}\right], \quad (1)$$

where C is the concentration of the diffusing substance, t is time, x is the spatial coordinate, D is the diffusion coefficient.

If the diffusion coefficient does not depend on the coordinate and time, then Eq. (1) takes the following form:

$$\partial C(x,t)/\partial t = D\partial^2 C(x,t)/\partial x^2. \quad (2)$$

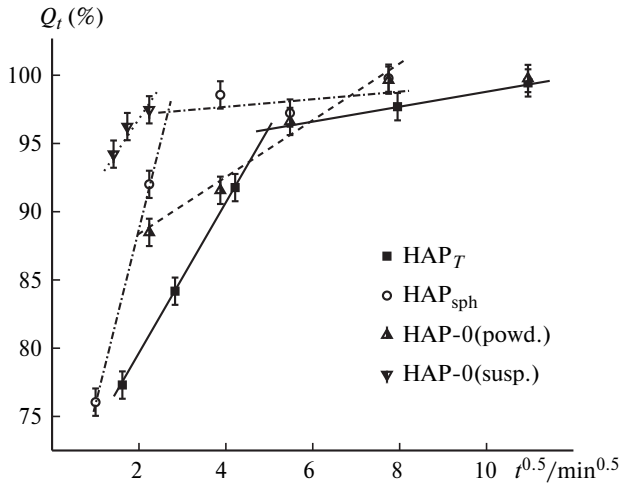

Fig. 7. Test for the presence off diffusion inside the particles during actinium sorption on various materials. In the case of HAP suspension, points in which sorption did not exceed 98% of the equilibrium value were used.

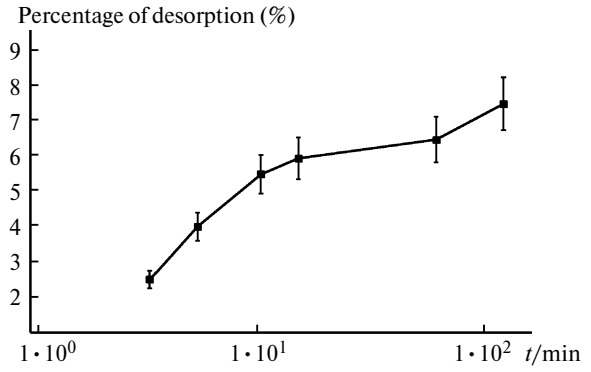

Fig. 8. Kinetics of actinium desorption from HAP; duration of the preliminary sorption is 1 h, pH 6.5.

For the initial condition $C(x,0) = M\delta(x)$ (M is the total amount of the added diffusing substance, $\delta(x)$ is the delta function) and an infinite layer, the problem solution is as follows:

$$C(x,t) = \frac{M}{\sqrt{4\pi Dt}} \exp\left[-x^2/(4Dt)\right]. \quad (3)$$

In our case, at the initial time point, a thin layer of actinium-containing solution is placed between the bases of two cylinders made of wet HAP paste. Actinium diffuses with time along the cylinder axes inside the HAP layer. This type of geometry is adequately described in an one-dimensional approximation, since deviation from this approximation is observed only near the lateral surface of the cylinder. However, this contribution is small because of the large radius of the cylinders. Furthermore, a real sorbent layer can also be considered infinite, in a first approximation, since the diffusing substance does not arrive to its boundary throughout the time of experiment. Thus, in our case, the penetration of diffusing actinium species in a layer of wet HAP paste is described by relation (3), where x is the distance along the cylinder axis, with the point 0 corresponding to the initial position of actinium. This dependence is linearized in the $\ln C$—x^2 or $\ln I$—x^2 coordinates, as the activity and the counting rate of the diffusing substance are proportional to its concentration:

$$\ln[I(x,t)] = -x^2/(4Dt) + \text{const}. \quad (4)$$

The effective diffusion coefficient can be found from the slope of the straight line that approximates the experimental distribution profile of the diffusing substance in the sorbent layer. Figure 9 shows this dependence for interpretation of the diffusion of actinium. The approximation parameters are as follows: $\ln(I) = -1.1 - 1.8x^2$ ($R^2 = 0.9193$). The calculated effective diffusion coefficient of actinium ions in a layer of wet HAP is $(1.0\pm0.2)\cdot10^{-7}$ cm^2 s^{-1}. This value is markedly higher than that obtained earlier for radium ions:[35] $(1.0\pm0.4)\cdot10^{-8}$ cm^2 s^{-1}. This difference is attributable to the influence of sorption—desorption processes on the kinetics of ion redistribution in the sorbent layer. In particular, radium, which is chemically similar to calcium, binds to the sorbent more strongly than actinium. As a result, the diffusion movement of actinium into the sorbent layer is less hindered than the movement of radium. Consequently, the effective diffusion coefficient is an order of magnitude higher for actinium than for radium.

Thus, the optimal conditions for the sorption of actinium(III) ions by HAP with various textures imply pH of the solution of 6—7 and the solid to liquid phase ratio of 20 mg of HAP per mL of the solution. The sorption kinetics studied under these conditions is well described by a pseudo-second-order model, and the model parameters found by calculations and the time it takes to reach

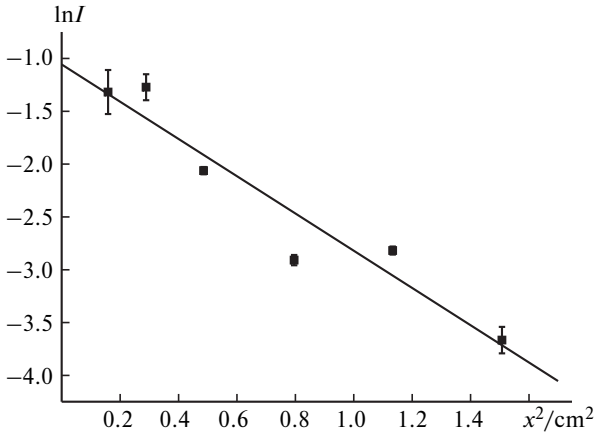

Fig. 9. Distribution of the actinium-225 in the sorbent layer after storage for 16 days; the dots correspond to experimental results and the line is approximation by relation (4). Approximation parameters: $\ln(I) = -1.1 - 1.8x^2$ ($R^2 = 0.9193$).

stationary sorption regime are correlated with the specific surface area and the porosity of HAP samples. The desorption of actinium in physiological saline is insignificant and amounts to 7—8%. Analysis of the kinetic dependences of sorption by textured HAP samples, that is, calcined powders and spheres, in terms of the Weber—Morris model showed the presence of a stage limited by internal diffusion. For estimating the diffusion coefficient of this process, an experiment was carried out in a special diffusion cell under conditions approaching the one-dimensional unsteady diffusion through a layer of wet HAP paste. The diffusion coefficient proved to be $(1.0\pm0.2)\cdot10^{-7}$ cm^2 s^{-1}. The obtained results can form the basis of development of a HAP-based transport system for a therapeutic ^{225}Ac radiopharmaceutical.

This work was financially supported by the Russian Foundation for Basic Research (Project No. 18-03-00432) and performed using research equipment of the Center for Collective Use of the Institute for Nuclear Research, Russian Academy of Sciences (contract with the Ministry of Education and Science No. 14.621.21.0014, unique identifier RFMEF162117X0014).

References

1. B. V. Egorova, O. A. Fedorova, S. N. Kalmykov, *Russ. Chem. Rev.*, 2019, **88**, 901.
2. L. Marcu, E. Bezak, B. Allen, *Critical Reviews in Oncology/Hematology*, 2018, **123**, 7.
3. A. Morgenstern, C. Apostolidis, F. Bruchertseifer, *Semin. Nucl. Med.*, 2020, **50**, 119.
4. M. Sathekge, F. Bruchertseifer, M. Vorster, I. O. Lawal, O. Knoesen, J. Mahapane, D. Cindy, R. Florette, A. Maes, C. Kratochwi, T. Lengana, L.F. Giesel, C. Van de Wiele, A. Morgenstern, *J. Nucl. Med.*, 2020, **61**, 62.

5. M. Sathekge, F. Bruchertseifer, O. Knoesen, *Eur J. Nucl. Med. Mol. Imaging*, 2019, **46**, 129.
6. F. Bruchertseifer, A. Kellerbauer, R. Malmbeck, A. Morgenstern, *J. Labelled Comp. Radiopharm.*, 2019, **62**, 794.
7. R. A. Aliev, S. V. Ermolaev, A. N. Vasiliev, V. S. Ostapenko, E. V. Lapshina, B. L. Zhuikov, N. V. Zakharov, V. V. Pozdeev, V. M. Kokhanyuk, B. F. Myasoedov, S. N. Kalmykov, *Solvent Extraction and Ion Exchange*, 2014, **32**, 468.
8. B. L. Zhuikov, *Appl. Radiat. Isotop*, 2014, **84**, 48.
9. K. John, *Eur. J. Nucl. Med. Mol. Imaging*, 2019, **46**, S722.
10. C. Hoehr, F. Bénard, K. Buckley, J. Crawford, A. Gottberg, V. Hanemaayer, P. Kunz, K. Ladouceur, V. Radchenko, C. Ramogida, A. Robertson, T. Ruth, N. Zacchia, S. Zeisler, P. Schaffer, *Phys. Procedia*, 2017, **90**, 200.
11. B. L. Zhuikov, S. N. Kalmykov, S. V. Ermolaev, R. A. Aliev, V. M. Kokhanyuk, V. L. Matushko, I. G. Tananaev, B. F. Myasoedov, *Radiochemistry*, 2011, **53**, 73.
12. S. V. Ermolaev, B. L. Zhuikov, V. M. Kokhanyuk, V. L. Matushko, S. N. Kalmykov, R. A. Aliev, I. G. Tananaev, B. F. Myasoedov, *Radiochim. Acta*, 2012, **100**, 223.
13. C. Apostolidis, R. Molinet, J. McGinley, *Appl. Radiat. Isotop*, 2005, **62**, 383.
14. C. Shih, L. Blok, R. Niederkohr, A. Avins, *J. Nucl. Med.*, 2019, **60**, 2041.
15. A. S. Sobolev, R. A. Aliev, S. N. Kalmykov, *Russ. Chem. Rev.*, 2016, **85**, 1011.
16. K. J. Harrington, S. Mohammadtah, P. S. Uster, D. Glass, A. M. Peters, J. S. Stewart, *Clin. Cancer Res.*, 20017, 243.
17. P. Datta, S. Ray, *J. Labelled Comp. Radiopharm.*, 2020; DOI: 10.1002/jlcr.3839.
18. L. Arazi, T. Cooks, M. Schmidt, Y. Keisari, I. Kelson, *Phys. Med. Biol.*, 2007, **52**, 5025.
19. S. B. Lee, H. W. Lee, T. D. Singh, *Theranostics*, 2017, **7**, 926.
20. J. Xie, K. Chen, J. Huang, *Biomaterials*, 2010, **31**, 3016.
21. J. V. Rojas, J. D. Woodward, N. Chen, A. J. Rondinone, C. H. Castano, S. Mirzadeh, *Nucl. Med. Biol.*, 2015, **42**, 614.
22. F. Chen, H. Hong, Y. Zhang, *Radiolabeled Mesopor. Silica Nanoparticles ACS Nano*, 2013, **7**, 9027.
23. N. Larson, H. Ghandehari, *Chem. Mater.*, 2012, **24**, 840.
24. K. K. Kamaleshwaran, D. Rajan, B. Krishnan, *Indian J. Nucl. Med.*, 2015, **30**, 47.
25. A. S. Shinto, K. K. Kamaleshwaran, S. Chakraborty, *World J. Nucl. Med.*, 2015, **14**, 81.
26. J. U. M. Calegaro, J. Machado, R. G. Furtado, *Haemophilia*, 2014, **20**, 421.
27. J. Gómez del Río, P. Sanchez, P. J. Morando, D. S. Cicerone, *Chemosphere*, 2006, **64**, 1015.
28. A. Yasukawa, T. Yokoyama, K. Kandori, T. Ishikawa, *Colloids Surf., A. Physicochem. Eng. Asp.*, 2007, **299**, 203.
29. A. G. Kazakov, A. V. Severin, *J. Radioanal. Nucl. Chem.*, 2020, **5**, 1.
30. A. V. Severin, I. A. Berezin, M. A. Orlova, T. P. Trofimova, A. Yu. Lupatov, A. V. Egorov, V. M. Pleshakov, *Russ. Chem. Bull.*, 2020, **69**, 665.
31. J. Kozempel, M. Vlk, E. Malkova, A. Bajzıkova, J. Barta, R. Santos-Oliveira, A. Malta Rossi, *J. Radioanal. Nucl. Chem.*, 2015, **304**, 443.
32. A. V. Severin, M. A. Orlova, E. S. Shalamova, *Russ. Chem. Bull.*, 2019, **68**, 2197.
33. P. Suchánková, E. Kukleva, K. Štamberg, P. Nykl, M. Sakmár, M. Vlk, J. Kozempel, *Materials*, 2020, **13**, 1915.
34. A. Vasiliev, A. Severin, E. Lapshina, E. Chernykh, S. Ermolaev, S. Kalmykov, *J. Radioanal. Nucl. Chem.*, 2017, **311**, 1503.
35. A. V. Severin, A. N. Vasiliev, A. V. Gopin, I. E. Vlasova, E. V. Chernykh, *Radiochemistry*, 2019, **61**, 339.
36. A. N. Vasiliev, Ph.D Thesis, M. V. Lomonosov Moscow State University, Moscow, 2016, 20 pp. (in Russian).
37. A. N. Vasiliev, V. S. Ostapenko, E. V. Lapshina, S. V. Ermolaev, S. S. Danilov, B. L. Zhuikov, S. N. Kalmykov, *Radiochimica Acta*, 2016, **104**, 539.
38. A. V. Severin, D. A. Pankratov, *Russ. J. Inorg. Chem.*, 2016, **61**, 265.
39. V. N. Rudin, V. F. Komarov, I. V. Melikhov, *Sposob polucheniya suspenzii gidroksiapatita* [*Method of Preparing Hydroxyapatite Suspension*], RF Patent No. 2122520, 1998.
40. E. I. Suvorova, V. V. Klechkovskaya, V. F. Komarov, A. V. Severin, *Crystallogr. Rep.*, 2006, **51**, 881.
41. A. V. Severin, V. F. Komarov, V. E. Bozhevol´nov, I. V. Melikhov, *Russ. J. Inorg. Chem.*, 2005, **50**, 72.
42. A. V. Severin, A. V. Gopin, A. N. Vasiliev, K. I. Enikeev, *Radiokhimiya* [*Radiochemistry*], 2020, **62**, No. 6 (in Russian).
43. R. Akkaya, *J. Radioanal. Nucl. Chem.*, 2012, **292**, 125.
44. M. Prasad, S. Saxena, *Indust. Eng. Chem. Res.*, 2004, **43**, 1512.
45. W. J. Weber, J. C. Morris, *J. Sanit. Eng. Div. Am. Soc. Civ. Eng.*, 1963, **89**, 31.
46. G. McKay, M. S. Otterburn, A. G. Sweeney, *Water Res.*, 1980, **14**, 15.
47. G. McKay, *J. Chem. Technol. Biotechnol.*, 1983, **33**A, 196.
48. F. C. Wu, R. L. Tseng, R. S. Juang, *Water Res.*, 2001, **35**, 613.
49. J. S. Suk, Q. Xu, N. Kim, J. Hanes, L. M. Ensign, *Adv. Drug Deliv. Rev.*, 2016, **99**, 28.
50. M. Hosseinzade, S. R. Karimi, A. Valian, H. Nojehdehian, *Biomed. Res.*, 2016, **27**, 442.
51. V. Lobaz, R. Konefał, J. Pánek, M. Vlk, J. Kozempel, M. Petřík, M. Hrubý, *Colloids Surf. B, Biointerfaces*, 2019, **179**, 143.
52. A. Morgenstern, C. Apostolidis, C. Kratochwil, M. Sathekge, L. Krolicki, F. Bruchertseifer, *Curr. Radiopharm.*, 2018, **11**, 200.

Received May 30, 2020;
in revised form July 27, 2020;
accepted September 1, 2020